ISSN: 0975-833X

Available online at http://www.journalcra.com

International Journal of Current Research
Vol. 11, Issue, 05, pp.3935-3940, May, 2019

DOI: https://doi.org/10.24941/ijcr.35467.05.2019

INTERNATIONAL JOURNAL OFCURRENTRESEARCH

RESEARCH ARTICLE

HUHS1015 REDUCES PKM2 PROTEIN DUE TO AUTOPHAGIC DEGRADATION IN GASTRIC CANCER CELLS

***Tomoyuki Nishizaki**

Research Director, Innovative Bioinformation Research Organization, Kobe, Japan

ARTICLEINFO

Article History:
Received 20th February, 2019
Received in revised form
17th March, 2019
Accepted 13th April, 2019
Published online 30th May, 2019

Key Words:
HUHS1015, PKM2,
Autophagic degradation,
Caspase, Apoptosis,
Gastric cancer cell.

ABSTRACT

The newly synthesized anticancer drug HUHS1015 decreased pyruvate kinase M2 (PKM2) protein in MKN28 and MKN45 human gastric cancer cells in a treatment time (10-60 min)-dependent manner. The effect of HUHS1015 was clearly inhibited by the autophagy inhibitor 3-methyladenine. HUHS1015 increased LC3-II, that is required for the autophagosome formation in the autophagic processes, in a treatment time (10-60 min)-dependent manner. PKM2 deficiency induces cell death including apoptosis and activated caspase-3, -4, -8, and -9. Taken together, the results of the present study show that HUHS1015 decreases PKM2 protein due to autophagic degradation, which contributes to caspase activation and apoptosis induction in MKN28 and MKN45 cells.

***Citation: Tomoyuki Nishizaki,* 2019.** "HUHS1015 reduces PKM2 protein due to autophagic degradation in gastric cancer cells", *International Journal of Current Research*, 11, (05), 3935-3940.

INTRODUCTION

The newly synthesized naftopidil analogue 1-[2-(2-methoxyphenylamino) ethylamino]-3-(naphthalene-1-yloxy)propan-2-ol (HUHS1015) induces apoptosis in a variety of cancer cells that include human malignant mesothelioma cells such as MSTO-211H, NCI-H28, NCI-H2052, and NCI-H2452 cell lines, human lung cancer cells such as A549, SBC-3, and Lu-65 cell lines, human hepatoma cells such as HepG2 and HuH-7 cell lines, human gastric cancer cells such as MKN28 and MKN45 cell lines, human colonic cancer cells such as Caco-2 and CW2 cell lines, human bladder cancer cells such as 253J, 5637, KK-47, TCCSUP, T24, and UM-UC-3 cell lines, human prostate cancer cells such as DU145, LNCaP, and PC-3 cell liens, and human renal cancer cells such as ACHN, RCC4-VHL, and 786-O cell lines (Kanno *et al*., 2013). As regarding gastric cancer cells, HUHS1015 induces caspase-independent apoptosis in MKN28 cells by accumulating apoptosis-inducing factor-homologous mitochondrion-associated inducer of death (AMID) accumulation in the nucleus (Kaku *et al*., 2015a). HUHS1015, on the other hand, induces caspase-dependent apoptosis in MKN45 cells by upregulating expression of tumor necrosis factor α (TNFα), a ligand of TNFα receptor involving activation of caspase-8 followed by the effector casepase-3 (Kaku *et al*., 2015b). HUHS1015 also induces caspase-dependent apoptosis in MKN45 cells by activating caspase-3 in association with mitochondrial damage, but without affecting release of cytochrome c, DIABLO, apoptosis-inducing factor (AIF), or AMID (Ohyama *et al*., 2015). Intriguingly, HUHS1015 promotes autophagic degradation of X-linked inhibitor of apoptosis protein (XIAP), thereby neutralizing caspase-3 inhibition due to XIAP, to activate caspase-3 and induce apoptosis in MKN45 cells (Nishizaki, 2016). The present study was conducted to gain further insight into the HUHS1015 actions in MKN28 and MKN45 gastric cancer cells. The results demonstrate that HUHS1015 reduces PKM2 protein due to autophagic degradation, at least in part responsible for caspase activation and apoptosis induction in MKN28 and MKN45 cells.

MATERIALS AND METHODS

Cell culture: MKN28 cells, a well differentiated human gastric adenocarcinoma cell line, and MKN45 cells, a poorly differentiated gastric adenocarcinoma cell line, were kindly gifted from Dr. Tatematsu (Nagoya University, Japan). Cells were plated and grown in a RPMI1640 solution (Sigma, St. Louis, MO, USA) supplemented with 10% heat-inactivated fetal bovine serum, penicillin (final concentration, 100 U/ml), and streptomycin (final concentration, 0.1 mg/ml) in a humidified atmosphere of 5% CO_2 and 95% air at 37°C.

Coomassie brilliant blue (CBB) staining: MKN28 cells were lysed in a lysis buffer [50 mM Tris–HCl, 150 mM NaCl, 0.1% (w/v) sodium deoxycholate, 0.1% (v/v) Triton X-100, and

protease inhibitor cocktail, pH 7.4] after 24-h treatment with and without HUHS1015 (100 μM). Then, lysates were loaded on 10% (v/v) sodium dodecyl sulfate-polyacrylamide gel electrophoresis (SDS-PAGE) and separated proteins were stained with CBB.

Matrix-assisted laser desorption ionization time of flight mass spectrometry (MALDI-TOFMS) analysis: The bands with a substantial decrease after HUHS1015 treatment in the CBB staining were excised and the amino acid sequence for each protein was analyzed with MALDI-TOFMS.

Knockdown of PKM2 protein: The siRNA to silence the PKM2-targeted gene was obtained from Santa Cruz Biotechnology (Santa Cruz, CA, USA) and the negative control (NC) siRNA from Ambion (Carlsbad, CA, USA). siRNAs were transfected into cells using a Lipofectamine reagent (Invitrogen, Carlsbad, CA, USA), and cells were used for experiments 48 h after transfection. To confirm successful knockdown, Western blotting was performed using antibodies against PKM2 antibody (Cosmo Bio, Tokyo, Japan) and β-actin (Cell Signaling, Beverly, MA, USA).

Western blotting: After treatment, cells were lysed and the lysates were loaded onto SDS-PAGE and transferred to polyvinylidene difluoride membrane. The blotting membrane was reacted with antibodies against PKM2 (Cosmo Bio, Tokyo, Japan), microtubule-associated protein light chain 3 (LC3) (Medical & Biological laboratories, Nagoya, Japan), and β-actin (Cell Signaling, Beverly, MA, USA), followed by a horseradish peroxidase (HRP)-conjugated anti-mouse IgG antibody. Immunoreactivity was detected with an ECL kit (Invitrogen, Carlsbad, CA, USA) and visualized using a chemiluminescence detection system (GE Healthcare, Piscataway, NJ, USA). Protein concentrations for each sample were determined with a BCA protein assay kit (Thermo Fisher Scientific, Rockford, IL, USA).

Real-time reverse transcription-polymerase chain reaction (RT-PCR): Total RNAs from cells were purified by an acid/guanidine/thiocyanate/chloroform extraction method using a Sepasol-RNA I Super kit (Nacalai, Kyoto, Japan). After purification, total RNAs were treated with RNase-free DNase I (2 units) at 37°C for 30 min to remove genomic DNAs, and 10 mg of RNAs was resuspended in water. Then, random primers, dNTP, 10× RT buffer, and Multiscribe Reverse Transcriptase were added to the RNA solutions and incubated at 25°C for 10 min followed by 37°C for 120 min to synthesize the first-strand cDNA. Real-time RT-PCR was performed using SYBR Green Realtime PCR Master Mix (Takara Bio) in the Applied Biosystems 7900 real-time PCR detection system (ABI, Foster City, CA, USA). Thermal cycling conditions were as follows: first step, 94°C for 4 min; the ensuing 40 cycles, 94°C for 1 s, 65°C for 15 s, and 72°C for 30 s. The primers used were as follows: (Forward) ATTGCCCGAGAGGCAGAGGC and (Reverse) ATCAAGGTACAGGCACTACACGCAT for PKM2; and (Forward) GACTTCAACAGCGACACCCACTCC and (Reverse) AGGTCCACCACCCTGTTGCTGTAG for glyceraldehyde 3-phosphate dehydrogenase (GAPDH). The quantity of the PKM2 mRNA was normalized by that of the GAPDH mRNA.

Cell viability: Cell viability was evaluated by the 3-(4,5-dimethyl-2-thiazolyl)-2,5-diphenyl-2*H*-tetrazolium bromide (MTT) method as previously described (Saitoh *et al*., 2004).

Enzymatic caspase assay: Caspase activity was measured using a caspase fluorometric assay kit (Ac-Asp-Glu-Val-Asp-MCA for a caspase-3 substrate peptide; Ac-Leu-Glu-Val-Asp-AFC for a caspase-4 substrate peptide; Ac-Ile-Glu-Thr-Asp-MCA for a caspase-8 substrate peptide, and Ac-Leu-Glu-His-Asp-MCA for a caspase-9 substrate peptide) by the method previously described (Yang *et al*., 2007). Briefly, cells were harvested and centrifuged at 1,200 rpm for 5 min at 4°C. The pellet was incubated in a cell lysis buffer on ice for 10 min and reacted with the fluorescently labeled tetrapeptide at 37°C for 2 h. The intensity of fluorescence was measured at an excitation wavelength of 380 nm and an emission wavelength of 460 nm for caspase-3, -8, and -9 or an excitation wavelength of 400 nm and an emission wavelength of 505 nm for caspase-4 with a fluorometer (Fluorescence Spectrometer, F-4500, Hitachi, Japan).

Apoptosis assay: Cells were suspended in a binding buffer and stained with both propidium iodide (PI) and annexin V (AV)-FITC, and loaded onto a flow cytometer (FACSCalibur; Becton Dickinson, Franklin Lakes, NJ, USA) available for FL1 and FL2 bivariate analysis. Data from 20,000 cells/sample were collected, and the quadrants were set according to the population of viable, unstained cells in untreated samples. CellQuest (Becton Dickinson) analysis of the data was used to calculate the percentage of the cells in the respective quadrants.

Statistical analysis: Statistical analysis was carried out using unpaired *t*-test and analysis of variance (ANOVA) followed by a Bonferroni correction.

RESULTS

PKM2 is a target of HUHS1015: My initial attempt was to probe the target proteins responsible for HUHS1015-induced cell death in MKN28 cells. In the CBB staining, a substantial decrease of the signal after 24-h treatment with HUHS1015 (100 μM) was detected in 6 bands (Fig. 1).

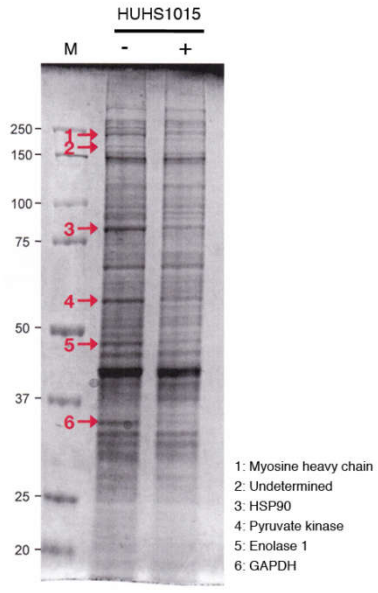

Figure 1. PKM2 is a target of HUHS1015.CBB staining was carried out in cell lysates from MKN28 cells treated without (-) and with (+) HUHS1015 (100 μM) for 24 h. Note a substantial decrease of 6 signal bands (1-6) after HUHS1015 treatment (arrows). M, marker. Proteins in the signal bands were analyzed using MALDI-TOFMS.

Each band was excised and analyzed with MALDI-TOFMS. Five of 6 bands were identified, corresponding to myosine heavy chain, heat shock protein 90 (HSP90), PKM2, enolase 1, and glyceraldehyde 3-phosphate dehydrogenase (GAPDH) (Figure 1). Of identified proteins PKM2 is recognized to play a role in cancer progression (Hsu *et al*., 2018; Li *et al*., 2018) and therefore, I have focused upon PKM2 as a target of HUHS1015.

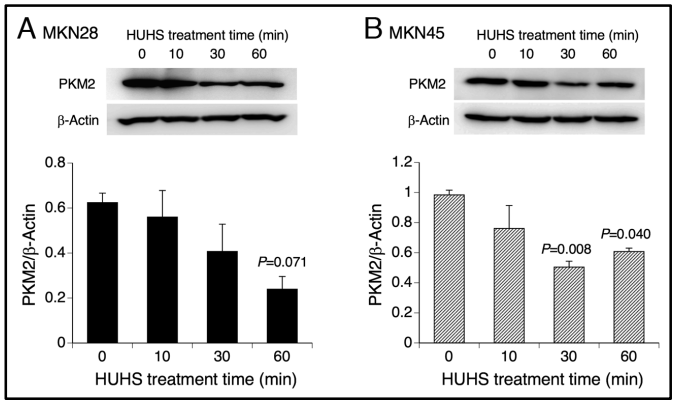

Figure 2. HUHS1015 decreases PKM2 protein in a treatment time-dependent manner. MKN28 (A) and MKN45 cells (B) were treated with HUHS1015 (HUHS) (100 μM) for periods of time as indicated, followed by Western blotting. In the graphs, each column represents the mean (± SEM) signal intensity for PKM2 relative to the intensity for β-actin (n=4 independent experiments). *P* values, ANOVA followed by a Bonferroni correction

HUHS1015 decreases PKM2 protein due to autophagic degradation: In the Western blot analysis, HUHS1015 (100 μM) decreased PKM2 protein in a treatment time (10-60 min)-dependent manner in MKN28 cells (Figure 2A). A similar effect was also obtained with MKN45 cells (Figure 2B). In the real-time RT-PCR analysis, HUHS1015 (100 μM) had no effect on the PKM2 mRNA levels through 10-60-min treatment in MKN28 cells (Figure 3A). This indicates that HUHS1015-induced decrease of PKM2 protein in MKN28 cells is not due to downregulation of PKM2 mRNA. For MKN45 cells, HUHS1015 (100 μM) did not affect the PKM2 mRNA levels through 10-30 min treatment, but a significant decrease was found at 60-min treatment (Figure 3B). This suggests that downregulation of PKM2 mRNA may in part contribute to HUHS1015-induced decrease of PKM2 protein in MKN45. Notably, HUHS1015-induced decrease of PKM2 protein in MKN28 and MKN45 cells was significantly prevented by 3-methyladenine (3-MA), an inhibitor of autophagy (Figure 4A,B). This suggests that HUHS1015 reduces PKM2 protein due to autophagic degradation in both the cell types. LC3 is required for autophagosome formation in the autophagic process (Padman*et al*., 2017). Cytoplasmic LC3 is processed by autophagy-related 4 (Atg4) protein, a cysteine protease, to produce LC3-I (Oikonomou*et al*., 2018). Then, LC3-I is covalently linked to phosphatidylethanolamine to form LC3-II (Oikonomou*et al*., 2018). LC3-II maturates autophagosome by depositing on the membrane (Oikonomou*et al*., 2018). The quantity of LC3-II and autophagosome formation have a positive correlation (Pugsley, 2017). Accordingly, autophagy can be assessed by monitoring the quantity of LC3-II. HUHS1015 (100 μM) increased LC3-II in parallel with decrease of LC3-I in a treatment time (10-60 min)-dependent manner in MKN28 cells (Figure 5A). A similar effect was also found with MKN45 cells (Figure 5B). These results further support the notion that HUHS1015 promotes autophagic degradation of PKM2 in MKN28 and MKN45 cells, leading to decrease of PKM2 protein.

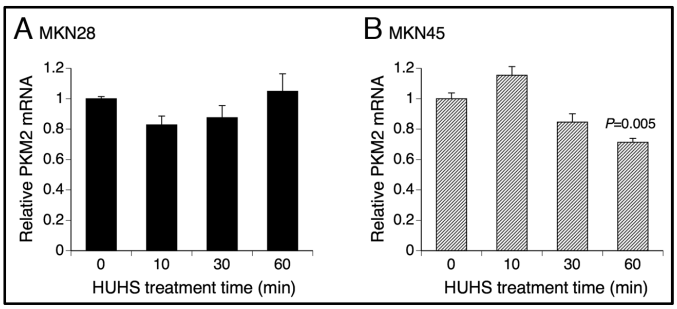

Figure 3. Effect of HUHS1015 on the PKM2 mRNA levels. MKN28 (A) and MKN45 cells (B) were treated with HUHS1015 (HUHS) (100 μM) for periods of time as indicated, followed by real-time RT-PCR. The quantity for the PKM2 mRNA was normalized by that for the GAPDH mRNA. In the graphs, each column represents the mean (± SEM) ratio relative to the normalized quantity for the PKM2 mRNA at 0 min (n=4 independent experiments). *P* value, ANOVA followed by a Bonferroni correction

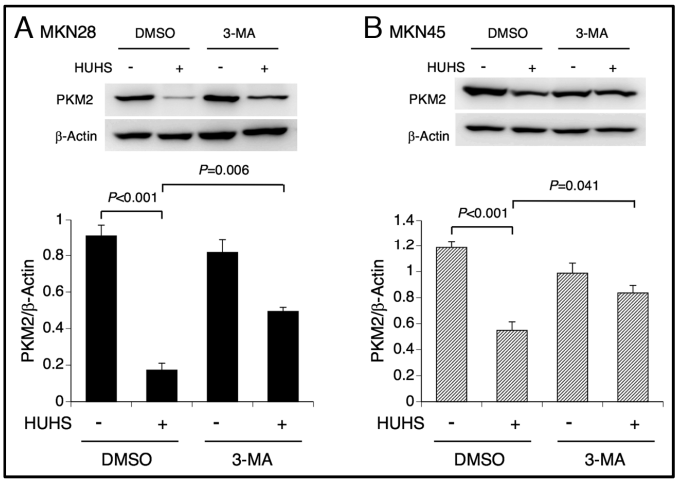

Figure 4. Autophagy is implicated in the HUHS1015-induced decrease of the PKM2 protein levels. MKN28 (A) and MKN45 cells (B) were treated with HUHS1015 (HUHS) (100 μM) for 60 min in the absence and presence of 3-MA (10 mM), followed by Western blotting. In the graphs, each column represents the mean (± SEM) signal intensity for PKM2 relative to the intensity for β-actin (n=4 independent experiments). *P* values, ANOVA followed by a Bonferroni correction

PKM2 deficiency initiates MKN28 and MKN45 cell death: It has been already established that HUHS1015 induces MKN28 and MKN45 cell death (Kaku *et al*., 2015a; Kakuet *al*., 2015b; Nishizaki, 2016; Ohyama *el al*., 2015). The question is whether decrease of PKM2 protein causes HUHS1015-induced cell death. To address this question, PKM2 protein was knocked-down. First of all, it was confirmed that PKM2 is successfully knocked-down in MKN28 and MKN45 cells by transfecting with the PKM2 siRNA (Figure 6A). Cell viability both in MKN28 and MKN45 cells was significantly lowered by knocking-down PKM2 (Figure 6B). This indicates that decrease of PKM2 protein is a factor to initiate MKN28 and MKN45 cell death.

PKM2 deficiency activates caspase-3, -4, -8, and -9 and induces apoptosis in MKN28 and MKN45 cells: In the enzymatic caspase assay, activities of caspase-3, -4, -8, and -9

in MKN28 cells were raised to 2.5 to 3.5 folds of the basal levels by knocking-down PKM2 (Figure 7A). Likewise, activities of caspase-3, -4, -8, and -9 in MKN45 cells were significantly raised by knocking-down PKM2 (Figure 7B). These findings indicate that PKM2 deficiency activates caspase-3, -4, -8, and -9 in MKN28 and MKN45 cells; conversely, PKM2 refrains activation of caspase-3, -4, -8, and -9 in MKN28 and MKN45 cells. PI is a marker of dead cells and AV is a marker of apoptotic cells (Vanags *et al*., 1996).

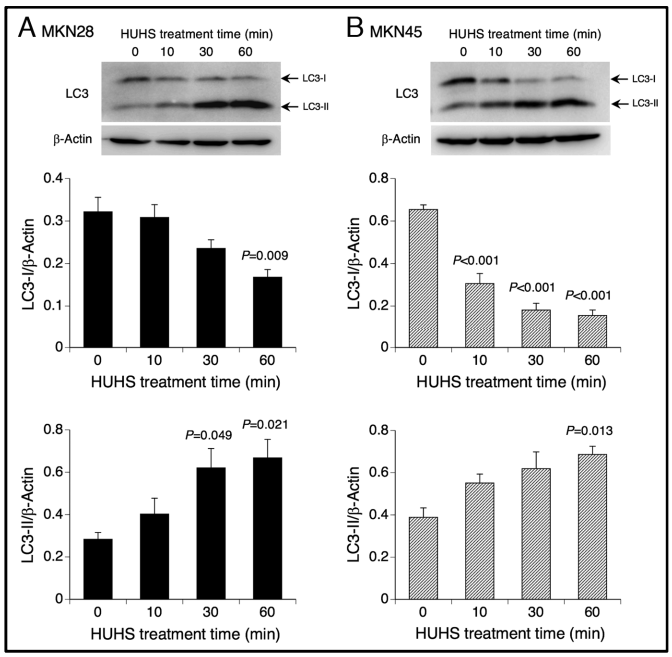

Figure 5.HUHS1015 increases LC3-II in parallel with decrease of LC3-I.MKN28 (A) and MKN45 cells (B) were treated with HUHS1015 (100 μM) for periods of time as indicated, followed by Western blotting. In the graphs, each column represents the mean (± SEM) signal intensity for LC3-I or LC3-II relative to the intensity for β-actin (n=4 independent experiments). *P* values, ANOVA followed by a Bonferroni correction

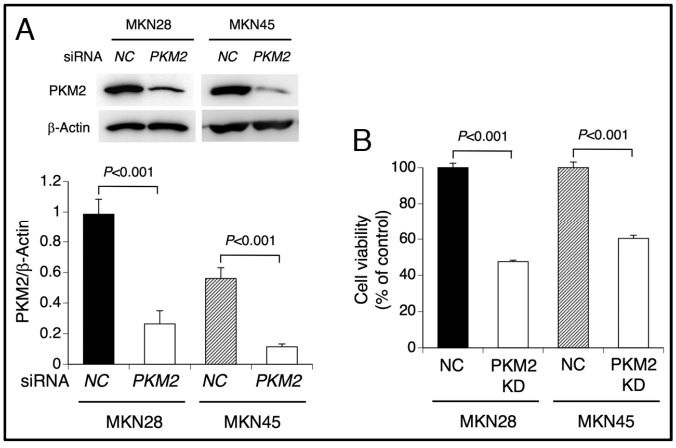

Figure 6. PKM2 deficiency reduces cell viability in MKN28 and MKN45 cells. (A) Cells were transfected with the PKM2 siRNA or the NC siRNA, and 48 h later Western blotting was carried out. In the graph, each column represents the mean (± SEM) signal intensity for PKM2 relative to the intensity for β-actin (n=4 independent experiments). *P* values, unpaired *t*-test. (B) MTT assay was carried out in cells 72 h after transfection with the PKM2 siRNA (PKM2 KD) or the NC siRNA (NC). In the graph, each column represents the mean (± SEM) percentage of control (MTT intensities of cells transfected with the NC siRNA) (n=4 independent experiments). *P* values, unpaired *t*-test.

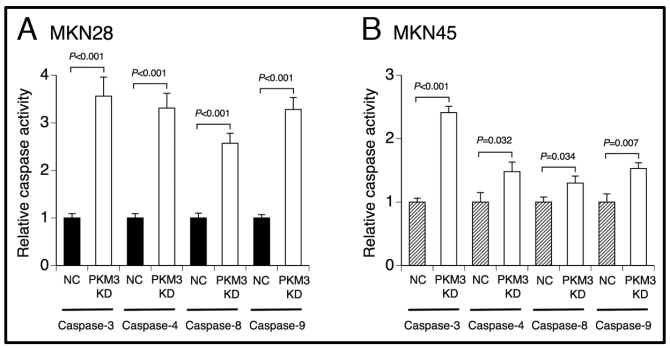

Figure 7. PKM2 deficiency activates caspase-3, -4, -8, and -9 in MKN28 (A) and MKN45 cells (B). Enzymatic caspase assay was carried out in cells 72 h after transfection with the PKM2 siRNA (PKM2 KD) or the NC siRNA (NC). In the graphs, each column represents the mean (± SEM) ratio relative to the caspase activity in cells transfected with the NC siRNA (n=4 independent experiments). *P* values, unpaired *t*-test

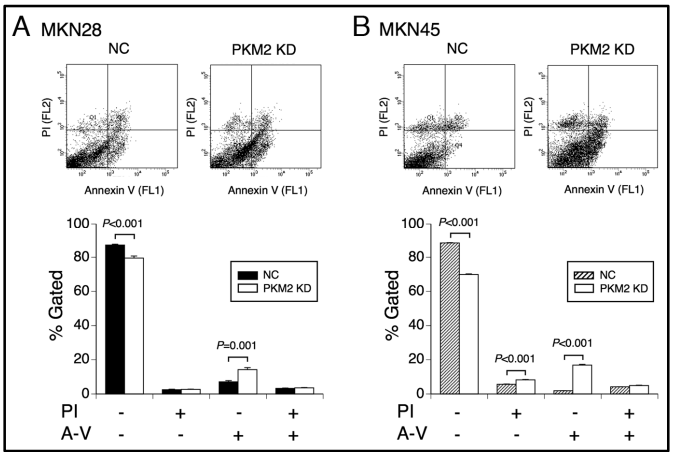

Figure 8. PKM2 deficiency induces apoptosis in MKN28 cells (A) and apoptosis/necrosis in MKN45 cells (B). Flow cytometry using PI and AV was carried out in cells 72 h after transfection with the PKM2 siRNA (PKM2 KD) or the NC siRNA (NC). In the graphs, each column represents the mean (± SEM) percentage of cells in 4 fractions against total cells (n=4 independent experiments). *P* values, unpaired *t*-test

In the flow cytometry using PI and AV, the population of PI-negative/AV-positive cells in MKN28 cells, corresponding to cells undergoing early apoptosis (Pietra *et al*., 2001), significantly increased in association with significant decrease in the populations of PI-negative/AV-negative cells, corresponding to alive cells, by knocking-down PKM2 (Figure 8A). For MKN45 cells, the populations of PI-positive/AV-negative and PI-negative/AV-positive cells, corresponding to cells undergoing primary necrosis and early apoptosis, respectively (Pietra *et al*., 2001), significantly increased in association with significant decrease in the populations of PI-negative/AV-negative cells by knocking-down PKM2 (Figure 8B). These results indicate that PKM2 deficiency induces apoptosis in MKN28 cells and necrosis/apoptosis in MKN45 cells.

DISCUSSION

In the present study, HUHS1015 decreased PKM2 protein in a treatment time (10-60 min)-dependent manner in MKN28 and MKN45 cells without affecting the PKM2 mRNA levels except for the decrease at 60-min treatment in MKN45 cells, and the effect was clearly inhibited by the autophagy inhibitor

3-MA. Moreover, HUHS1015 increased LC3-II, that is required for the autophagosome formation in the autophagic processes (Pugsley, 2017), in parallel with decrease of LC3-I in a treatment time (10-60 min)-dependent manner in MKN28 and MKN45 cells. Taken together, these results indicate that HUHS1015 decreases PKM2 protein mainly due to autophagic degradation in both the cell types. In the earlier study, HUHS1015 also decreased XIAP protein due to autophagic degradation in MKN45 cells (Nishizaki, 2016). HUHS1015, thus, appears to promote autophagy. Of particular interest is the finding that cell viability in MKN28 and MKN45 cells was definitely lowered by knocking-down PKM2. This indicates that decrease of PKM2 protein could be a factor for HUHS1015-induced cell death. Activities of caspase-3, -4, -8, and -9 in MKN28 and MKN45 cells were markedly raised by knocking-down PKM2. This explains that decrease of PKM2 protein is implicated in the activation of caspase-3, -4, -8, and -9, to induce apoptosis. In the flow cytometry using PI and AV, the population of PI-negative/AV-positive cells in MKN28 cells, corresponding to cells undergoing early apoptosis (Pietra *et al*., 2001), and the populations of PI-positive/AV-negative and PI-negative/AV-positive cells in MKN45 cells, corresponding to cells undergoing primary necrosis and early apoptosis, respectively (Pietra *et al*., 2001), significantly increased in association with significant decrease of the populations of PI-negative/AV-negative cells, corresponding to alive cells, by knocking-down PKM2. This implies that decrease of PKM2 protein induces apoptosis in MKN28 cells and necrosis/apoptosis in MKN45 cells. Overall, the results presented here allow drawing a conclusion that HUHS1015 decreases PKM2 protein due to autophagic degradation, which contributes to caspase activation and initiation of apoptosis in MKN28 and MKN45 cells. The results also suggest that decrease of PKM2 protein may be also implicated in the initiation of necrosis in MKN45 cells.

Pyruvate kinase generates ATP when phosphoenolpyruvate is converted to pyruvate. The ATP generation by pyruvate kinase is independent from oxygen supply, allowing survival of the organs under hypoxic conditions as seen in solid cancers (Vaupel and Harrison, 2004). PKM2, that diverts glucose-derived carbon from catabolic to biosynthetic pathways, is present in most cancers (Steinberg *et al*., 1999) and expression of PKM2 is upregulated in cancer cells (Christofk *et al*., 2008; Hamabe *et al*., 2014). PKM2 plays a role in cancer progression through both metabolic and non-metabolic pathways (Hsu *et al*., 2018; Li *et al*., 2018). Nuclear PKM2 promotes progression of oral squamous cell carcinoma by inducing epithelial-mesenchymal transition and post-translationally repressing transforming growth factor β (TGF-β)-induced factor homeobox 2 (Tanaka *et al*., 2018). Expression of PKM2 correlates with progression of oral squamous cell carcinoma in association with production of reactive oxygen species (ROS) and integration of glutamine into lactate (Kurihara-Shimomura *et al*., 2018). Accumulating evidence has pointed to the critical role of PKM2 in the oncogenesis, progression, and prognosis of gastric cancer (Lim *et al*., 2012; Shiroki *et al*., 2017). A study shows a link between PKM2 and E-cadherin during epidermal growth factor (EGF) receptor-stimulated gastric cancer cell motility and invasion (Wang *et al*., 2013). Overexpression of PKM2 and hexokinase 1 associates with lymphatic metastasis, advanced clinical staging and unfavorable prognosis in gastric cancer (Gao *et al*., 2015). Expression of PKM2 was upregulated by cytotoxin-associated gene A, a pathogenic factor of *Helicobacter pylori*, through an extracellular signal-regulated kinase (ERK) pathway, in part responsible for carcinogenesis and development of gastric cancer (Shiroki *et al*., 2017). PKM2, alternatively, facilitates gastric cancer cell migration through a phosphatidylinositol 3-kinase (PI3K)/Akt pathway (Wang *et al*., 2017). Based upon these data, a recent interest focuses on targeting PKM2 as a potential therapeutic strategy in the treatment for gastric cancer. PKM2 promotes aerobic glycolysis that cancer cells favor. A change into aerobic glycolysis-dependent metabolism is referred to as the 'Warburg effect', a vital hallmark of cancer cells. LY294002, a PI3K inhibitor, inhibits the Warburg effect in gastric cancer cells by downregulating PKM2 and exhibits an anticancer effect on gastric cancer (Lu *et al*., 2018). Overexpression of microRNA-let-7a suppresses proliferation, migration, and invasion of gastric cancer cells by downregulating expression of PKM2 (Tang *et al*., 2016). Pantoprazole, a proton pump inhibitor, inhibits human gastric adenocarcinoma SGC-7901 cells by downregulating expression of PKM2 (Shen *et al*., 2016). Combination treatment using shikonin, a PKM2 inhibitor, and BPTES, a glutaminase inhibitor, exhibits a beneficial anticancer effect on hypoxia-resistant gastric cancer cells (Kitayama *et al*., 2017). Metformin inhibits gastric cancer via the inhibition of hypoxia inducible factor 1α/PKM2 signaling (Chen *et al*., 2015). A variety of drugs targeting PKM2, thus, have been developed for treatment of gastric cancer. HUHS1015 targets PKM2 in gastric cancer cells by the mechanism distinct from that for any drug previously developed and therefore, HUHS1015 could become a novel promising drug for treatment of gastric cancer.

Conclusion

The results of the present study show that HUHS1015 decreases PKM2 protein due to autophagic degradation, to activate caspase-3, -4, -8, and -9 and induce apoptosis in MKN28 and MKN45 cells. This may extend our understanding about the anticancer actions of HUHS1015.

REFERENCES

Chen, G., Feng, W., Zhang, S., *et al*. 2015. Metformin inhibits gastric cancer via the inhibition of HIF1α/PKM2 signaling. *Am. J. Cancer Res.,* 5:1423-1434.

Christofk, H.R., Vander Heiden, M.G., Wu, N., *et al*. 2008. Pyruvate kinase M2 is a phosphotyrosine-binding protein. Nature, 452:181-186.

Gao, Y., Xu, D., Yu, G., *et al*. 2015. Overexpression of metabolic markers HK1 and PKM2 contributes to lymphatic metastasis and adverse prognosis in Chinese gastric cancer. *Int. J. Clin. Exp. Pathol.,* 8:9264-9271.

Hamabe, A., Konno, M., Tanuma, N., *et al*. 2014. Role of pyruvate kinase M2 in transcriptional regulation leading to epithelial-mesenchymal transition. *Proc. Natl. Acad. Sci. U.S.A.,* 111:15526-15531.

Hsu, M.C., Hung, W.C. 2018. Pyruvate kinase M2 fuels multiple aspects of cancer cells: from cellular metabolism, transcriptional regulation to extracellular signaling. Mol. Cancer, 17:35.

Kaku, Y., Tsuchiya, A., Kanno, T., *et al*. 2015a. HUHS1015 induces necroptosis and caspase-independent apoptosis of MKN28 human gastric cancer cells in association with AMID accumulation in the nucleus. *Anticancer Agents Med. Chem.,* 15:242-247.

Kaku, Y., Tsuchiya, A., Kanno, T., *et al*. 2015b. The newly synthesized anticancer drug HUHS1015 is useful for treatment of human gastric cancer. *Cancer Chemother. Pharmacol.,* 75:527-535.

Kanno, T., Tanaka, A., Shimizu, T., *et al*. 2013. 1-[2-(2-Methoxyphenylamino)ethylamino]-3-(naphthalene-1-yloxy)propan-2-ol as a potential anticancer drug. Pharmacology, 91:339-345.

Kitayama, K., Yashiro, M., Morisaki, T., *et al*. 2017. Pyruvate kinase isozyme M2 and glutaminase might be promising molecular targets for the treatment of gastric cancer. *Cancer Sci.,* 108:2462-2469.

Kurihara-Shimomura, M., Sasahira, T., Nakashima, C., *et al*. 2018. The multifarious functions of pyruvate kinase M2 in oral cancer cells. *Int. J. Mol. Sci.,* 19(10). pii: E2907.

Li, Y.H., Li, X.F., Liu, J.T., *et al*. 2018. PKM2, a potential target for regulating cancer. Gene, 668:48-53.

Lim, J.Y., Yoon, S.O., Seol, S.Y., *et al*. 2012. Overexpression of the M2 isoform of pyruvate kinase is an adverse prognostic factor for signet ring cell gastric cancer. *World J. Gastroenterol.,* 18:4037-4043.

Lu, J., Chen, M., Gao, S., *et al*. 2018. LY294002 inhibits the Warburg effect in gastric cancer cells by downregulating pyruvate kinase M2. *Oncol. Lett.,* 15:4358-4364.

Nishizaki, T. 2016. HUHS1015 promotes autophagic XIAP degradation to induce apoptosis of gastrointestinal cancer cells. *Ind. J. Med. Res. Pharmaceut. Sci.,* 8:8-17.

Ohyama, M., Kaku, Y., Tsuchiya, A., *et al*. 2015. HUHS1015 induces apoptosis of MKN45 gastric cancer cells by activating caspase-3 in association with mitochondrial damage. *Int. J. Biol. Pharm. Res.,* 6:771-775.

Oikonomou, V., Renga, G., De Luca, A., *et al*. 2018. Autophagy and LAP in the fight against fungal infections: Regulation and therapeutics. Mediators Inflamm., 2018:6195958.

Padman, B.S., Nguyen, T.N., Lazarou, M. 2017. Autophagosome formation and cargo sequestration in the absence of LC3/GABARAPs. Autophagy, 13:772-774.

Pietra, G., Mortarini, R., Parmiani, G., *et al*. 2001. Phases of apoptosis of melanoma cells, but not of normal melanocytes, differently affect maturation of myeloid dendritic cells. *Cancer Res.,* 61:8218-8226.

Pugsley, H.R. 2017. Quantifying autophagy: Measuring LC3 puncta and autolysosome formation in cells using multispectral imaging flow cytometry. *Methods* 112:147-156.

Saitoh, M., Nagai, K., Nakagawa, K., *et al*. 2004. Adenosine induces apoptosis in the human gastric cancer cells via an intrinsic pathway relevant to activation of AMP-activated protein kinase. *Biochem. Pharmacol.,* 67:2005-2011.

Shen, Y., Chen, M., Huang, S., *et al*. 2016. Pantoprazole inhibits human gastric adenocarcinoma SGC-7901 cells by downregulating the expression of pyruvate kinase M2. Oncol. Lett., 11:717-722.

Shiroki, T., Yokoyama, M., Tanuma, N., *et al*. 2017. Enhanced expression of the M2 isoform of pyruvate kinase is involved in gastric cancer development by regulating cancer-specific metabolism. *Cancer Sci.,* 108:931-940.

Steinberg, P., Klingelhöffer, A., Schäfer, A., *et al*. 1999. Expression of pyruvate kinase M2 in preneoplastic hepatic foci of N-nitrosomorpholine-treated rats. *Virchows Arch.,* 434:213-220.

Tanaka, F., Yoshimoto, S., Okamura, K., *et al*. 2018. Nuclear PKM2 promotes the progression of oral squamous cell carcinoma by inducing EMT and post-translationally repressing TGIF2. *Oncotarget,* 9:33745-33761.

Tang, R., Yang, C., Ma, X., *et al*. 2016. MiR-let-7a inhibits cell proliferation, migration, and invasion by down-regulating PKM2 in gastric cancer. *Oncotarget.,* 7:5972-5984.

Vanags, D.M., Pörn-Ares, M.I., Coppola, S., *et al*. 1996. Protease involvement in fodrin cleavage and phosphatidylserine exposure in apoptosis. *J. Biol. Chem.,* 271:31075-31085.

Vaupel, P., Harrison, L. 2004. Tumor hypoxia: causative factors, compensatory mechanisms, and cellular response. Oncologist, 9 Suppl 5:4-9.

Wang, C., Jiang, J., Ji, J., *et al.* 2017. PKM2 promotes cell migration and inhibits autophagy by mediating PI3K/AKT activation and contributes to the malignant development of gastric cancer. *Sci. Rep.,* 7:2886.

Wang, L.Y., Liu, Y.P., Chen, L.G., *et al*. 2013. Pyruvate kinase M2 plays a dual role on regulation of the EGF/EGFR signaling via E-cadherin-dependent manner in gastric cancer cells. *PLoS One,* 8:e67542.

Yang, D., Yaguchi, T., Yamamoto, H., *et al*. 2007. Intracellularly transported adenosine induces apoptosis in HuH-7 human hepatoma cells by downregulating c-FLIP expression causing caspase-3/-8 activation. *Biochem. Pharmacol.,* 73:1665-1675.

****